Ocean Engineering 287 (2023) 115926

Contents lists available at ScienceDirect

Ocean Engineering

journal homepage: www.elsevier.com/locate/oceaneng

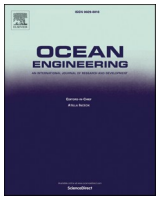

An investigation on the effect of widespread internal corrosion defects on the collapse pressure of subsea pipelines

Michael Olatunde, Srinivas Sriramula, M. Amir Siddiq, Alfred R. Akisanya *

School of Engineering, University of Aberdeen, Aberdeen, AB24 3UE, UK

ARTICLE INFO

Handling Editor: Prof. A.I. Incecik

Keywords:
Collapse pressure
Corroded pipe
Decommissioning

ABSTRACT

Deepwater subsea pipelines are an essential part of offshore oil and gas infrastructure, and it is a statutory requirement for operators to monitor the degradation of pipelines left-in-place at cessation of production. Collapse is one of the failure modes for subsea pipelines subjected to external pressure. Surface corrosion defects in subsea pipelines, either while still operational or after cessation of production, usually manifest as widespread or localized corrosion pits that are randomly spread on the steel surface. Extensive work has been done on predicting the collapse pressure of pipelines containing single corrosion defects however, the same cannot be said for randomly distributed corrosion defects. In this study, we investigate, for the first time, the effects of the geometry and coverage extent of widespread internal corrosion defects with random spatial distribution on the collapse pressure of pipelines using finite element analysis. The results show that corrosion defect depth and coverage surface area are the main defect geometric parameters that significantly influence the collapse strength of pipelines with randomly distributed internal corrosion. An empirical function for predicting the collapse pressure of a corroded pipeline is developed to reduce the need for recurrent computational effort.

1. Introduction

Oil and gas drilling and production infrastructures are decommissioned at the cessation of production with some of the infrastructure left-in-place. Post decommissioning monitoring for the structural integrity of the left-in-place offshore infrastructure, e.g., subsea pipelines, is a statutory requirement (Bureau Veritas, 2018; ODU OPRED BEIS, 2018). The corrosion of sealed left-in-place deepwater pipelines and the consequent impact on the collapse strength need to be accurately predicted for safe and efficient structural monitoring of the pipelines. The collapse of pipelines, with and without geometric imperfections, has been extensively studied in literature. Two of the most widely studied geometric imperfections for circular cylindrical pipes are the ovality, Δ_o, which is a measure of out-of-roundness of the pipe, and thickness eccentricity, Ξ_o, which is a measure of non-uniformity of the wall thickness. The ovality, Δ_o, and eccentricity, Ξ_o, illustrated in Fig. 1, are related to the diameter and wall thickness according to (Chen et al., 2022; Li et al., 2022; Netto et al., 2007; Sakakibara et al., 2008):

$$\Delta_o = \frac{D_{max} - D_{min}}{D_{max} + D_{min}} \tag{1}$$

$$\Xi_o = \frac{t_{max} - t_{min}}{t_{max} + t_{min}} \tag{2}$$

where $D_{\max}$ and $D_{\min}$ are the maximum and minimum outer diameters of the pipe respectively, and $t_{\max}$ and $t_{\min}$ are the maximum and minimum wall thickness of the pipe respectively.

He et al. (2014) used finite element analysis (FEA) to investigate the effects of ovality, yield stress and material anisotropy on the collapse pressure of thick-walled steel pipelines and observed that D/t ratio, initial ovality and yield stress have significant effects on collapse response of pipelines. Subsequent work by Zhang and Pan (2020) considered the effect of wall thickness eccentricity and a wider range of ovalities and showed that the collapse mode is a function of the interaction between the ovality and thickness eccentricity. Fallqvist (2009) performed a comprehensive study on the effect of geometry (D/t), geometric imperfections (ovality, eccentricity, peaking and flattening), boundary conditions, material models, residual stresses, and radial and circumferential variations in material properties on the collapse pressure of thick-walled pipelines using FEA. Their study revealed that localised imperfections are more detrimental to collapse pressure compared to eccentricity and that ovality is the most influential

* Corresponding author.
E-mail address: a.r.akisanya@abdn.ac.uk (A.R. Akisanya).

https://doi.org/10.1016/j.oceaneng.2023.115926
Received 20 May 2023; Received in revised form 23 August 2023; Accepted 25 September 2023

geometric imperfection as regards the collapse pressure of uncorroded pipelines. Extensive work has been carried out by other researchers on the effect of geometric imperfections on the collapse pressure of uncorroded pipes, see, for example, Assanelli et al. (2000), Gong et al. (2013), Kara et al. (2010), Ramasamy and Tuan Ya (2014), and Yu et al. (2019). Here and thereafter, D and t are respectively the nominal outer diameter and wall thickness of the pipe.

There have been few studies on the effect of corrosion and other surface defects on the collapse pressure of pipes. Xue and Hoo Fatt (2002) developed an analytical model for predicting the collapse pressure of a circular cylinder with a reduced wall thickness over a section of the circumference and compared the analytically determined collapse pressures to the results from finite element analysis. The collapse pressure was found to decrease with increasing thickness reduction and circumferential coverage. Sakakibara et al. (2008) investigated the effect of the geometry of a single internal corrosion defect, idealized as a rectangular axial groove, on the collapse pressure of corroded pipelines. Netto et al. (2007) studied the effect of the geometric characteristics of a single external corrosion defect on the collapse pressure of pipelines subject to external pressure using a combination of small-scale experiments and finite element analysis. It was observed that the coincidence of the defect position with the most compressed region of the ovalised pipe had the most detrimental effect on the collapse strength of the pipe. Netto (2009, 2010) developed a simple model for estimating the collapse pressure of pipelines containing narrow external corrosion defects and subjected to external pressure. Zhang et al. (2020) investigated the effect of non-symmetrical corrosion defect on the collapse pressure of subsea pipelines using a simplified model based on the work of Netto et al. (2007) and observed that collapse pressure may decrease with increased corrosion defect length, width, or depth if the circumferential coverage of the collapse is small due to the interaction between ovality and the defect geometry.

It is clear from these earlier studies that in addition to the typical geometric, material and loading factors that determine the collapse pressure of uncorroded pipelines, the collapse pressure of corroded pipelines is affected by the geometry (Netto et al., 2007; Netto, 2009, 2010; Xue and Hoo Fatt, 2002) and coverage (Wang et al., 2018a, 2018b) of the corrosion defects. However, most of the previous studies on the effect of corrosion defects on collapse pressure have focused on isolated single defect and on thin-walled pipes, e.g., Kara et al. (2010) and Ramasamy and Tuan Ya (2014). The finite element analysis of the collapse pressure of moderately thick-walled corroded pipelines have mostly been restricted to the use of solid continuum finite elements (Fallqvist, 2009; He et al., 2014; Zhang and Pan, 2020). For thin-walled pipes, the mesh resolution required to achieve converged results when solid continuum finite elements are used becomes significantly computationally disadvantageous compared to shell finite elements. This is because of the considerable deformation that is required before collapse, especially because of the number of elements along the thickness (radial direction).

Some researchers have presented the successful use of the shell element for buckling analysis of thick-walled cylinders. Sadowski and Rotter (2013) reported that thick shell finite elements can be used to successfully model the buckling of thick cylinders with $D/t = 19.5$ with inelastic behaviour. van den Berg (1995) developed a finite strain shell model for the accurate prediction of the deformation of moderately thick-walled ($10 < D/t < 100$) circular cylindrical pipelines without corrosion defects under the effect multiple load types including external pressure. It was noted that the results compared quite well with analytical, experimental and numerical work presented by others (Corona and Kyriakides, 1988; Ju and Kyriakides, 1992; Klever, 1992; Stanley, 1985; van Keulen, 1994; Yeh and Kyriakides, 1986). Hauch and Bai (2000) used general-purpose shell elements to perform the finite element analysis to validate the analytical equation developed for $10 < D/t < 60$.

Idealised single defects, as presented by the researchers above, seldom occur in operational or left-in-place decommissioned subsea pipelines. Although, corrosion geometry and spatial distributions on pipelines are usually random (Mansoori et al., 2017; Murer and Buchheit, 2013; Valor et al., 2007; Witek, 2021), very few researchers have focused on the effect of geometry and coverage intensity of multiple defects with random spatial distribution on the collapse pressure of pipelines under external pressure. Wang et al. (2018a, 2018b) investigated the effect of external corrosion pits with random spatial distribution on the collapse pressure of pipelines. The studies were performed with a combination of experiments and finite element analyses. The effect of the length of the pitting region and the pitting density were found to be the most influential parameters on the collapse pressure of the pipeline. Due to the use of anti-corrosion external coating and cathodic protection, internal corrosion defects are more common in subsea pipelines (Wu et al., 2022).

There is currently no explicit guidance in the public domain that addresses the effect of randomly distributed widespread internal corrosion on the collapse behaviour of externally pressurised pipelines. With the increasing number of pipelines entering decommissioning phase, pipelines that are left-in-place after decommissioning will be filled with seawater, and as a result, the internal surfaces of the pipelines become more susceptible to corrosion or corrosion exacerbation particularly due to microbiologically induced corrosion (MIC) because of the lack of product flow under pressure. It has therefore become relevant to understand how multiple internal corrosion defects would affect the collapse pressure of pipelines subject to external overpressure

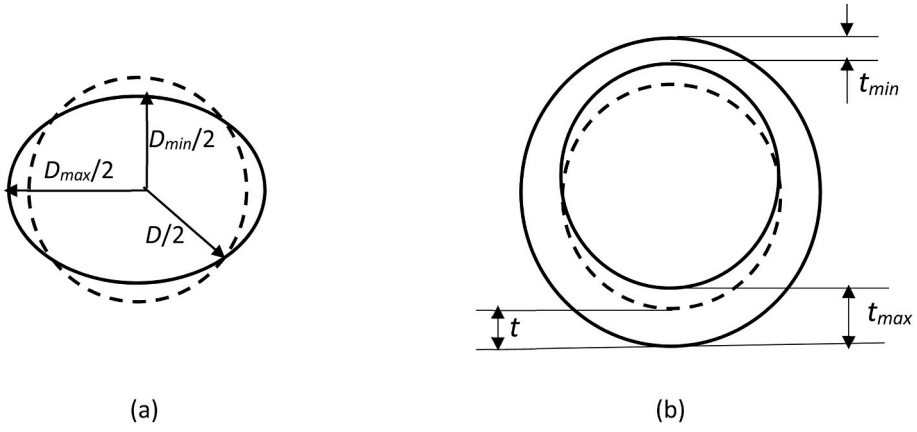

Fig. 1. Illustration of geometric imperfections in a circular pipe with a nominal outer diameter D: (a) ovality and (b) eccentricity. The dashed-dashed line is the perimeter of the pipe without imperfection, while the solid continuous line is the perimeter of the pipe with geometric imperfections.

in the post-operational phase to facilitate proper monitoring of out-of-use pipelines in the interim pipeline regime.

The current paper aims to bridge the knowledge gap in studying, for the first time, the effect of widespread internal corrosion defects with random surface distribution on the collapse pressure of pipelines. Nonlinear finite element analysis is used to investigate the effect of internal surface defect dimensions (size and depth) and area coverage on the characteristic collapse pressure of pipelines subject to external overpressure. The finite element results are used to develop an empirical model of the collapse pressure as a function of the significant geometric parameters of the corrosion defects and pipeline. The empirical model can then be utilised to perform reliability analyses of deteriorating pipelines for decision making in decommissioning and late life management. This is particularly the case for deep sea pipelines that have been decommissioned, plugged, and left in place on the seabed which require monitoring and inspection prior to final action such as operational reuse for carbon capture or ecological reuse for provision of substrate for reefs.

2. Methodology

The aim of the current research is to assess the effect of internal corrosion defects with random spatial distribution on the collapse pressure of circular cylindrical pipes subject to external pressure. The methodology adopted is as follows: (i) The material properties of the pipe are determined; (ii) a finite element model is developed, validated, and used to perform a parametric study of the effects of the geometric and spatial coverage characteristics of internal corrosion defects on collapse pressure, and; (iii) a non-linear regression analysis is then performed to develop a performance function for predicting the collapse pressure of deteriorating subsea pipelines.

2.1. Material properties

The pipelines considered in this study are assumed to be made from API 5 L X65. Solid circular cylindrical specimens for uniaxial tensile tests were machined from an API 5 L X65 pipeline. The tensile specimens had a diameter of 6 mm, and a gauge length of 40 mm. Tensile tests were carried out at room temperature (approximately 20 °C) in displacement control at a nominal strain rate of 4.17×10^{-4} s^{-1}. The test was performed using Instron model 4483 universal testing machine.

A representative measured uniaxial stress – strain response is shown in Fig. 2. The average material properties for three nominally identical specimens were: yield stress, $\sigma_y = 501$ MPa; tensile strength, $\sigma_{uts} = 601$ MPa; Young's Modulus, $E = 224$ GPa, and strain at σ_{uts}, $\epsilon_{uts} = 6.25\%$.

We note that the measured stress-strain response can be fitted to a linear elastic/linear hardening constitutive law:

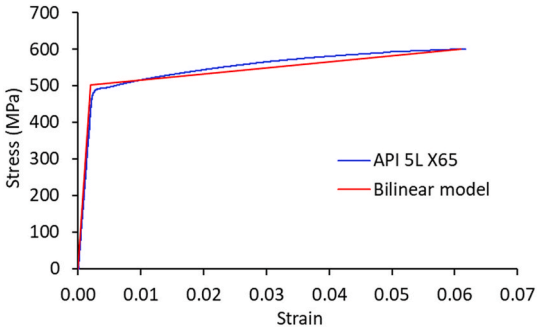

Fig. 2. Bilinear constitutive material model fitted to experimentally measured true uniaxial stress-strain response of API 5 L X65 specimen.

$$\sigma = \begin{cases} E\varepsilon & \text{for } \varepsilon \le \varepsilon_y \\ \sigma_y + H\varepsilon_p & \text{for } \varepsilon > \varepsilon_y \end{cases} \tag{3}$$

where ε_y (= 0.2%) is the yield strain, ε_p is the plastic strain, and H (=1.7 GPa) is the plastic modulus. The constitutive law (3) with the material properties stated above agrees well with the measured uniaxial stress – strain response, see Fig. 2. The finite element analysis of the collapse pressure was therefore carried out using the bi-linear constitutive law (3) with the measured material properties and a Poisson ratio $\nu = 0.3$.

2.2. Model development and validation

2.2.1. Failure criterion

The commercial software Abaqus (Dessault-Systemes, 2019) was employed for performing the FEA in this study. Abaqus has been extensively used by other researchers for collapse pressure analysis (He et al., 2014; Sadowski et al., 2017; Sadowski and Rotter, 2013; Wang et al., 2018b; Zhang and Pan, 2020). Localised buckling is a stability problem, therefore, all the FEA in this study were run by applying uniform external pressure incrementally using a modified arc length method (Crisfield, 1981) to trace the equilibrium path of the force-displacement curve. The failure criterion adopted is such that collapse is deemed to have occurred once the maximum sustainable external pressure is reached. This is in line with the previous limit point for collapse pressure detection used by Netto et al. (2007) and Wang et al. (2018b). Collapse is assumed to have occurred upon the satisfaction of (4) and (5):

$$\left|\frac{\partial \bar{I}^n}{\partial \bar{u}^m}\right| = |\mathbb{K}^{nm}| = 0, \tag{4}$$

$$\Delta\lambda_i < 0, \tag{5}$$

where $\mathbb{K}^{nm}$ is the tangent stiffness of the assembly, $\bar{I}^n$ are the internal forces, $\bar{u}^m$ are nodal displacements $\bar{u}$, n and m are the degree of freedom of the internal forces and displacements, respectively, and $\Delta\lambda_i$ is the increment in load proportionality factor λ_{i-1} towards the next load increment.

2.2.2. Element type selection

Before performing the parametric studies of the collapse pressure of pipe with randomly distributed internal corrosion defects, it was necessary to verify that the choice of element type could accurately replicate the results from existing standard analytical models (Det Norske Veritas, 2012), experiments and numerical models (Netto et al., 2007; Sakakibara et al., 2008). In previous studies, 8-node solid continuum element with reduced integration (C3D8R) (Fallqvist, 2009; He et al., 2014; Jin, 2016; Zhang and Pan, 2020) and 4-node doubly-curved shell element with reduced integration (S4R) (Hauch and Bai, 2000; Liang et al., 2020; Sadowski and Rotter, 2013) have been used for numerical analysis of the collapse behaviour under external pressure and global buckling of both thick-walled and thin-walled pipelines. Hence, these elements are considered in the validation and mesh convergence exercise to select the most appropriate finite element for the current study.

Corrosion defect-free pipes with $10 < D/t < 50$, an ovality of 0.5% (Det Norske Veritas, 2012), and axial length, $L = 5D$ (Fallqvist, 2009; Sakakibara et al., 2008) were modeled using the S4R and C3D8R elements from the ABAQUS elements library. The radial and translational axial degrees of freedom were kept free at one end of the pipe to simulate an infinite pipeline and an axial symmetry was applied at the other end, see Figs. 3 and 4. The ovality was applied through uniform ellipticity along the whole axial length of the pipe.

A mesh resolution of 40 elements around the circumference and 30 elements along the axial direction was used for the shell-based FE

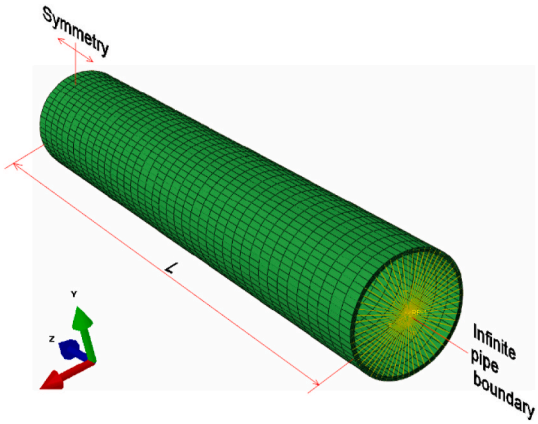

Fig. 3. FEA model of a defect free pipe with $D = 80$ mm, $D/t = 30$, using 60, 40 and 5 C3D8R elements along circumferential, axial and radial directions respectively.

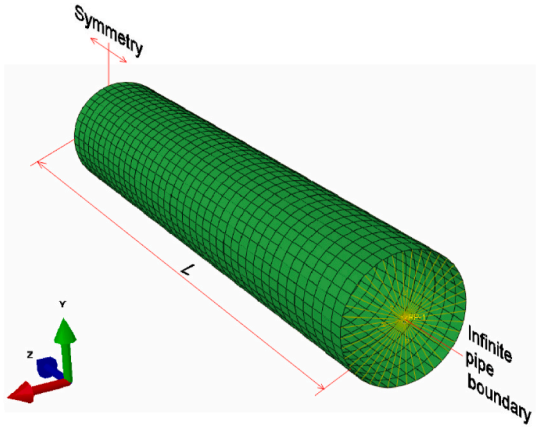

Fig. 4. FEA model of a defect-free pipe with $D = 80$ mm, $D/t = 30$, using 40 and 30 S4R elements along circumferential and axial directions respectively.

models (Fig. 4) after performing mesh sensitivity analyses. The shell elements had 5 integration points through the thickness. A similar approach was used by other researchers (Fallqvist, 2009) to successfully attain converged results. On the other hand, to achieve converged results for the solid-continuum-elements-based (SCE) FE models, 40 elements around the circumference and 30 elements along the axial direction were used for $D/t \leq 20$, while 50, 60, 80 and 100 elements around the circumference and 40 elements along the axial direction were used for D/t of 25, 30, 40 and 50 respectively upon the confirmation of mesh convergence. All SCE models had 5 elements across the thickness. The collapse pressures determined using the FEA models of the intact API 5 L X65 pipes modeled with S4R and C3D8R elements are shown in Fig. 5 along with the collapse pressures determined using the analytical equation (De Winter 1981; Det Norske Veritas, 2012) for elastic-plastic collapse under uniform external pressure. The analytical collapse pressure, P_c, for a circular cylinder pipe with nominal outer diameter D and wall thickness t, made from a material with Young's modulus, E, Poisson's ratio, ν, and subject to external pressure is given by (Det Norske Veritas, 2012)

$$\left(\frac{P_c}{P_e}-1\right)\left(\frac{P_c^2}{P_y^2}-1\right)=\frac{P_c}{P_e}.2\Delta_o.\frac{D}{t}, \tag{6}$$

where Δ_o is the ovality defined in (1),

$$P_e=\frac{2E}{1-\nu^2}\left(\frac{t}{D}\right)^3, \tag{7a}$$

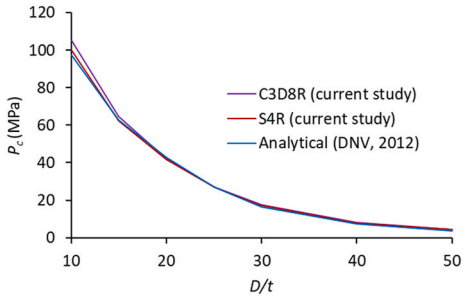

Fig. 5. Comparison of analytical and FE solutions of the collapse pressure of corrosion defect-free API 5 L X65 pipe using shell (S4R) and solid (C3D8R) elements.

$$P_y=\sigma_y\frac{2t}{D}\ . \tag{7b}$$

The results for both types of elements agree well with those of the analytical model. However, the FE model built with S4R shell elements required much fewer degrees of freedom and hence was more computationally time efficient to analyse. Consequently, the S4R element was selected for performing all subsequent FEA in this study.

2.2.3. *Pipelines with single isolated internal defect*

As part of the validation and mesh sensitivity analysis of our FE model, we compared the FE results from the current FEA with existing results for pipelines with a single axially oriented corrosion defect on the internal surface spanning the entire length of the pipe. The FE models were built with S4R elements and compared to a previous experimental and numerical study by Sakakibara et al. (2008). The circumferential sweep angle 2φ of the defect, thickness at defect t_w, ovality Δ_0, thickness eccentricity Ξ_o and the pipe geometry data used in the analysis were taken from Sakakibara et al. (2008) and are given in Table 1 for completeness. The determined collapse pressures are also given in Table 1. The same boundary conditions were used for this model as described in section 2.2.2 for pipes without defect.

The normalised collapse pressures obtained from the FE analysis in this study are in close agreement with those from the analytical and experimental work of Sakakibara et al. (2008), see Fig. 6. We compare the FEA results of the collapsed pressure from the current study with the corresponding experimental results by Sakakibara et al. (2008). We observed that the average mean square error from the current study is 60% less than the mean square error obtained when Sakakibara et al. (2008) FEA results are compared with their experimental results. This verifies the suitability of the shell-based FE model and the adopted failure criterion for determining the onset of collapse of partially internally corroded pipes.

2.2.4. *Pipes with random spatially distributed internal defects: parametric study*

The collapse of pipes with random spatially distributed internal defects and subject to external pressure, which has not previously been considered, is examined in the current study in line with level 3 assessment of remaining strength (American Petroleum Institute, 2016). We consider API 5 L X65 pipes with nominal internal diameter of 38.13 mm, outer diameter-to-thickness ratio in the range $10 \leq D/t \leq 30$ which covers the range for deep and ultra-deep-sea pipeline design (He et al., 2014) and ovality $\Delta_0 = 0.25\%$ (according to eq. (1)) - the minimum allowed in subsea pipelines by standard practice (Det Norske Veritas, 2012). In all the cases considered, the thickness eccentricity $\Xi_o = 0$. The internal corrosion defects are assumed to be square-shaped with defect length, c, depth, d, and total internal surface coverage area of the defect, A_d. The relative defect length with respect to the pipe internal circumference of $0 \leq c/\pi D_i \leq 0.05$, relative defect depth of $0 \leq d/t \leq 0.5$, and

Table 1
Geometric parameters of pipeline with internal defects and the collapse pressure taken from Sakakibara et al. (2008) and the corresponding results of the validation from the current study.

Pipe no	D (mm)	t (mm)	t_w (mm)	2φ	Δ_o (%)	Ξ_o %	Sakakibara et al.'s experiment	Sakakibara et al.'s FEA	Current study's FEA
							Collapse pressure (MPa)		
20	50.92	2.76	2.76	0	0.08	4.24	31.42	30.10	30.38
34	50.93	2.73	2.18	6	0.09	2.24	27.08	26.40	26.24
24	50.85	2.72	2.14	10	0.1	2.06	25.48	24.90	25.34
23	50.85	2.73	2.12	20	0.12	2.42	24.79	23.75	24.35
25	50.92	2.71	2.17	30	0.15	2.16	24.66	23.79	24.58
36	50.9	2.74	2.15	40	0.2	2.55	24.06	23.34	24.31
26	50.95	2.71	2.36	30	0.1	2.56	26.93	26.06	26.53
25	50.92	2.71	2.17	30	0.15	2.16	24.66	23.79	24.58
27	50.99	2.72	1.93	30	0.13	2.2	21.70	21.60	22.09
29	50.99	2.73	1.62	30	0.17	2.57	19.91	18.93	19.31
30	50.98	2.72	1.38	30	0.21	2.68	18.08	17.07	17.51
33	50.85	2.73	1.18	30	0.26	3.47	16.82	15.68	16.00

$E = 206$ GPa, $\sigma_y = 266$ MPa, power-law strain hardening index, $n = 0.076$.

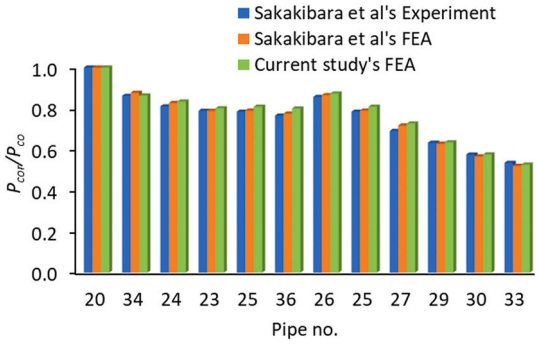

Fig. 6. Comparison of current FEA results of normalied collapse pressure for 12 different pipes containing internal corrosion with different values of circumferential sweep angle and depth with the corresponding experimental and numerical results by Sakakibara et al. (2008). The geometric parameters of the pipes are provided in Table 1.

nominal relative defect surface area coverage $A_c = \frac{A_d}{\pi D_i L}$ in the range $0 \leq A_c \leq 0.5$ where D_i is the nominal inner diameter and L is the length of the pipe were considered for the parametric study. The range of the relative defect length and relative defect depth was adopted to cover assumed long term corrosion defect dimensions. The range of defect coverage is adopted based on consideration that random pitting corrosion coverage beyond 50% of the surface area of the pipe tends towards uniform corrosion as will be discussed later.

A custom MATLAB script was used to generate and mesh the finite element models to ease automation. The random spatial distributions of the corrosion defects on the internal surface were imposed by randomly selecting locations on the discretised surface area of the pipeline with the *randsample* function in MATLAB (2021). The function was used in the model generation script to return locations of selected elements on the internal surface of the pipeline by sampling uniformly at random without replacement until the target area of defect coverage is achieved, see Fig. 7. The defect locations were random while the length and depth of the defects were kept uniform for each model instance. The reference surfaces of the shell finite elements were moved from the mid-thickness surface to the external surface of the pipe. The movement of the reference surface to the external surface of the pipe allows for the modelling of internal surface corrosion defects by varying the thickness of the shell elements with respect to the external surface of the FE pipeline models. Furthermore, this allows for the application of external pressure loading directly to external surface. The application of pressure loading without adjusting the location of the reference surface would result in the loading being applied on the mid-thickness surface of the pipe and an overestimation of the collapse pressure.

As with the validation model, the length of the pipe considered was $L = 5D$. A fixed boundary condition was applied at one end of the pipe and axial symmetry conditions at the other. The same material constitutive model as stated in section 2.1 was used. To adequately capture the planned size of the defects, a mesh resolution of 100 S4R elements around the circumference of the pipe was adopted. The input files for the FE models were generated with MATLAB and a Python script was used to automate the FE analysis in ABAQUS. Each run was terminated upon the detection of a drop in external pressure in accordance with the failure criterion described in section 2.2.1 and a new run commenced. In total, 505 numerical models were run to ensure a full factorial study for the parameter levels considered.

The collapse pressure values determined from the parametric study were curve fitted using a non-linear regression analysis to develop an

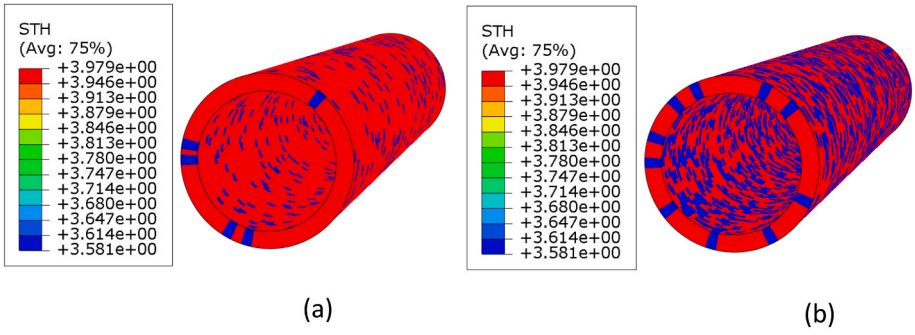

Fig. 7. Thickness contour (mm) of the generated pipeline FE models showing the distribution of the corrosion defects (in blue) for (a) low defects coverage, $A_c = 0.1$, and (b) high defects coverage, $A_c = 0.5$.

empirically enhanced model for predicting the collapse pressure of the deteriorating pipelines subject to evolving randomly spaced widespread corrosion defects as a function of the defect geometric parameters. The *fitnlm* (*fit nonlinear regression model)* function in MATLAB (2021) was used for this purpose. The function estimates the model coefficients of the specified function by employing an iterative procedure (Seber and Wild, 2003). The predictors (pitting geometry and coverage) and corresponding responses (collapse pressures) are provided as the input matrix and vector respectively. The size of the predictor matrix is the number of observations by the number of predictor variables. The dimension of the response vector is equal to the number of observations. A default exponential function with unknown coefficients was specified and initial trial values were supplied to initiate the iterations. An exponential approximation function was adopted based on the trend observed in the results of the FEA analysis.

3. Results and discussion

In practical scenarios, widespread corrosion defects on a pipeline surface are randomly located. The experiment performed by Wang et al. (2018a) corroborates the inherent spatial randomness of widespread corrosion defects. The interaction amongst the geometric parameters for an ovalised pipe with defects of random spatial distribution is complex. The collapse pressure of a pipeline is a function of the interaction between the circumferential and axial bending rigidities (Wang et al., 2018b). To undertake a realistic study of predicting the effect of widespread corrosion defects on pipeline characteristic collapse pressure, an extensive parametric analysis was performed to predict the effect of randomly distributed internal corrosion defects of increasing degrees of coverage based on the parameters and ranges specified in section 2.2.4.

3.1. Effect of D/t on normalised collapse pressure $\frac{P_{cor}}{P_c}$

The effect of the D/t ratio on the normalised collapse pressure $\frac{P_{cor}}{P_c}$ is shown in Fig. 8 for different values of relative defect coverage A_c and different relative defect length $c/\pi D_i$. The collapse pressure P_{cor} of a pipeline with defects has been normalised by the corresponding collapse pressure for a defect-free pipe P_c, given in eqn. (6) and shown in Fig. 5. Although P_c decreases with increasing D/t (see Fig. 5), we note that $\frac{P_{cor}}{P_c}$ for a given $c/\pi D_i$, d/t, and A_c is independent of D/t for $A_c \leq 0.2$, and decreases slightly with increasing D/t for $0.2 < A_c \leq 0.5$. For example, for $c/(\pi D_i) = 0.03$, $d/t = 0.3$ and $A_c = 0.5$, the normalised collapse pressure, $\frac{P_{cor}}{P_c}$, is found to be 0.76 when D/t = 10 and 0.71 when D/t = 30. The results shown in Fig. 8 indicate that the effect of D/t cancels out in the normalised collapse pressure.

3.2. Effect of defect length on normalised collapse pressure $\frac{P_{cor}}{P_c}$

The normalised collapse pressure remains almost constant for the range of relative corrosion defect lengths $c/\pi D_i$ considered as shown in Fig. 9. For the uniform square shaped defects considered in this study, we note that the defect size has little or no effect on the normalised collapse pressure. The slight variation in the values of $\frac{P_{cor}}{P_c}$ for $D/t \geq 20$ is attributed to the random spatial distribution of defects for the range of $c/\pi D_i$ values analysed. Although high defect coverage area ($A_C > 0.4$) may result in the significant overlap or coalescence of some of the initial uniformly sized defects, we conclude that the normalised collapse pressure of pipelines subject to multiple internal uniform square corrosion defects is not a direct function of the individual corrosion defect lengths.

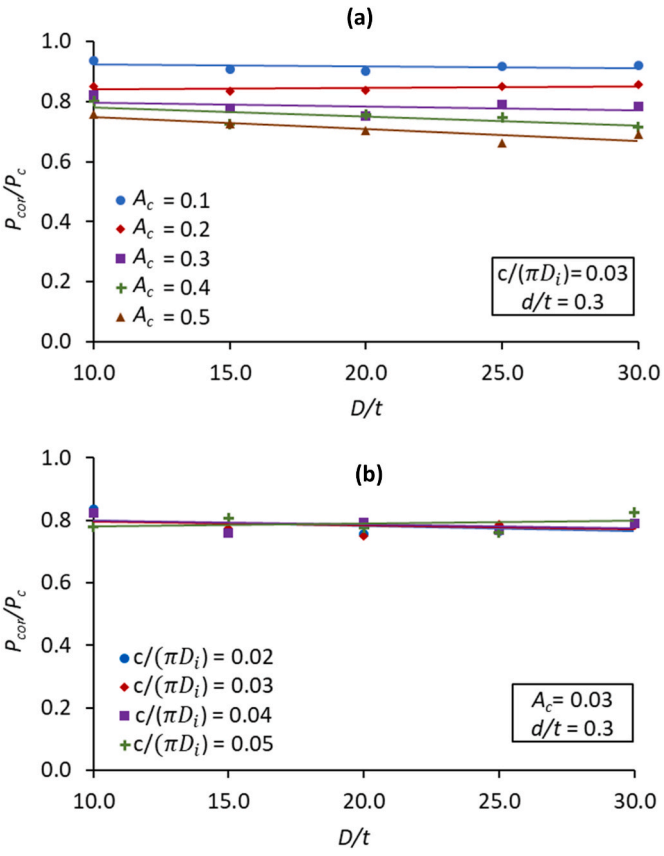

Fig. 8. Normalised collapsed pressure as function of D/t for (a) different relative defect coverages A_C, and (b) different relative defect lengths $c/(\pi D_i)$. P_c is the corresponding collapse pressure for a defect-free pipe.

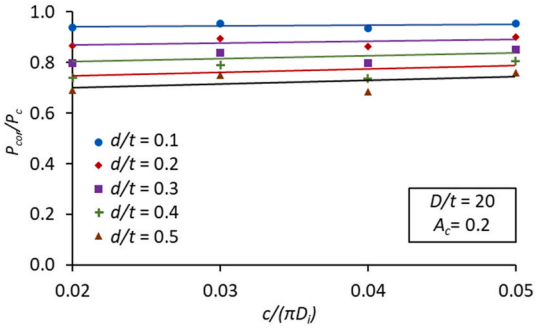

Fig. 9. Normalised collapsed pressure as a function of relative defect length $c/(\pi D_i)$ *for different relative defect depths* d/t. P_c is the corresponding collapse pressure for a defect-free pipe.

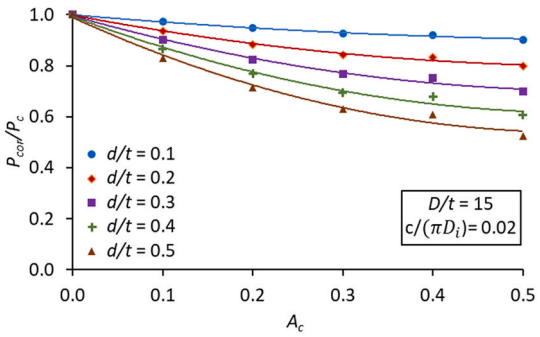

Fig. 10. Normalised collapsed pressure as a function relative surface coverage area of the defect A_c. P_c is the corresponding collapse pressure for a defect-free pipe.

3.3. Effect of relative defect coverage surface area on normalised collapse pressure $\frac{P_{cor}}{P_c}$

The effect of the relative coverage surface area of the defects on collapse pressure is non-linear as shown in Fig. 10. The relative collapse pressure decreases with increasing relative surface area coverage of the defect, A_c. We note that there is insignificant change in the relative collapse pressure as A_c increases beyond 0.4, because as the relative coverage area of the defects increases, more defects coalesce and/or overlap. As A_c increases, there is increased likelihood of more defects overlapping and connecting with each other to form a large enough single defect leading to localized collapse at the defect independently of the rest of the pipeline, see Fig. 11. A related analytical study performed by Xue and Hoo Fatt (2002) for pipelines with non-uniform wall thickness and verified using FEM analysis. It was demonstrated in the study that when a region of the pipeline has a sufficiently lower stiffness compared to the rest of the pipeline, the region effectively becomes a circular shell with built in ends, leading to localized collapse.

Thus, the defective section of the pipeline can collapse independently of the rest of the pipeline. Once this limit is reached, the collapse pressure becomes constant irrespective of any further progression in corrosion coverage surface area. In other studies (Netto et al., 2007; Sakakibara et al., 2008), similar observations have been made that increasing the coverage area of single corrosion defect (both internal and external) beyond a certain value yielded no further decrease in the normalised collapse pressure. Our results show similar trends corroborating past observations that there is a limit to collapse pressure decrease due to the coverage area of defects while other geometric properties are constant.

3.4. Effect of relative defect depth on normalised collapse pressure $\frac{P_{cor}}{P_c}$

The normalised collapse pressure decreases linearly with increasing relative defect depth (Fig. 12). The reduction in the collapse pressure with increasing relative defect depth increases with increasing relative surface coverage area A_c up to a limit, beyond which further increase in defect coverage yields no further reduction in the magnitude of the collapse pressure. The normalied collapse pressure versus d/t for A_c = 0.4 and 0.5 coincide; this corroborates the flattening trend as shown in Fig. 10. The results shown in Fig. 12 are consistent with a previous study by Sakakibara et al. (2008) where collapse pressure was found to decrease linearly with defect depth, and Wang and Shenoi (2019) where the magnitude of strength reduction varies under different defect coverages.

3.5. Effects of defect geometric parameters on collapse mode

The extent to which the collapse mode of a pipe is affected by the spatially random defects depends on whether the collapse is an elastic or yield collapse. In general, the collapse mode is more affected by surface defects when the pipe collapses by yielding as the collapse mode shape and orientation are influenced by the location of the plastic hinges formed. For defect-free pipelines without thickness eccentricity, the collapse mode shape is a function of the wave number of the imposed initial out-of-roundness imperfection and is independent of the D/t value of the pipe, i.e., it is independent of whether the collapse is achieved by yielding or elastic deformation. In the current study, an initial out-of-roundness imperfection with uniform amplitude across the length of the pipe and a wave number of 2 (synonymous to ovality) was imposed for all the analyses performed. This is the specification for collapse pressure determination by DNV Standard (Det Norske Veritas, 2012). An initial imperfection with a wave number of 2 results in a worst-case scenario for collapse pressure capacity because of the less efficient distribution of stresses around the pipe material circumference.

As the post collapse behaviour of the pipes is not considered in this

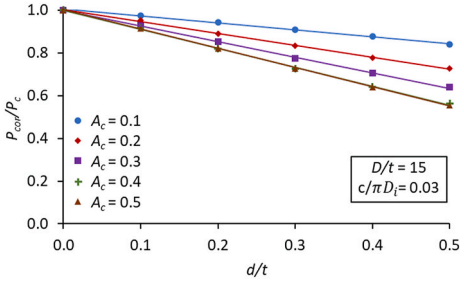

Fig. 12. Normalised collapsed pressure as function of relative defect depth d/t. P_c is the corresponding collapse pressure for a defect-free pipe.

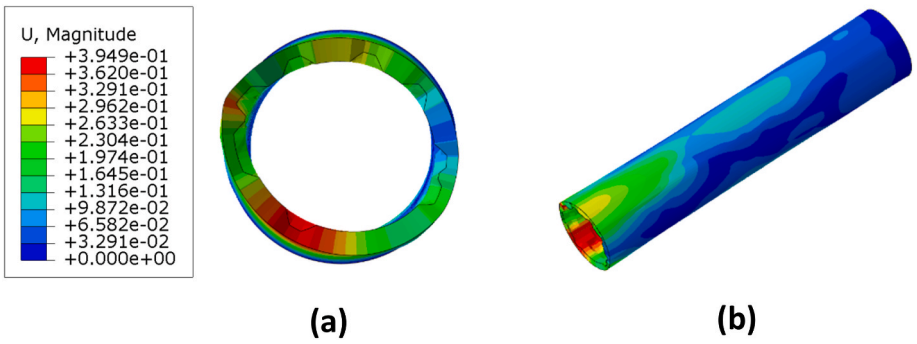

Fig. 11. Contour of the displacement (in mm) of the collapsed pipeline showing localised collapse of region with clustered corrosion defects for $\frac{D}{t} = 10, A_c = 0.5$, $\frac{c}{\pi D_i} = 0.04, \frac{d}{t} = 0.5$. (a) Cross-section of the pipe, and (b) 3D pipe geometry.

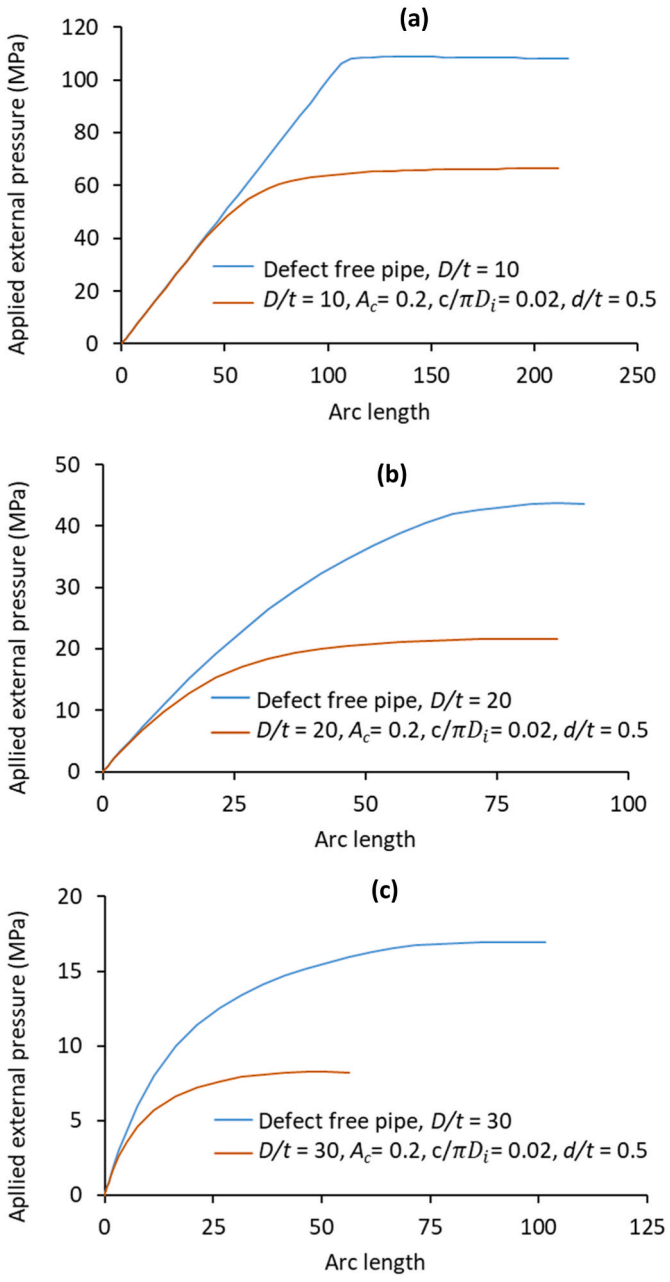

Fig. 13. External pressure - arc length response for 'Defect-free pipe' and 'Pipes with internal surface defects' (a) $D/t = 10$, (b) $D/t = 20$ and (c) $D/t = 30$.

study, the ∞ shaped collapse shape is not achieved as typical with post collapsed sections. Notwithstanding, the maximum attainable pressure as shown in Fig. 13 is reached in agreement with the failure criterion discussed in section 2.2.1.

It is useful to review the collapse mode of defect-free pipes collapse as this lays a basis for better understanding of the collapse mode of pipes with randomly distributed surface defects. For a defect-free pipe, the plastic hinges coincide with the major and minor axis as shown by the contour of the effective plastic strain in Fig. 14.

We observed that the collapse mode shape for pipelines with internal surface defects is not significantly influenced by the length of the individual defects and the overall relative coverage of the defects, see Fig. 15. However, the collapse mode shape is significantly influenced by the combined effects of the D/t value, defect depth, and circumferential location of the defects. For shallow corrosion defects ($d/t = 0.1$) on low D/t pipes (i.e., $D/t \leq 20$), irrespective of the relative area of defect coverage, the plastic hinges that dictate the mode of yield collapse are formed at or close to the minor and major axes as in defect-free pipes. Although the plastic hinges formed are not evenly distributed due to the randomness of the defects imposed (see the Appendix), the imposed initial out-of-roundness imperfection still dictates the collapse mode just as for defect-free pipes.

For deep defects ($d/t \geq 0.3$) with low D/t (≤ 20) values, plastic hinges can be preferably formed at other locations other than along the minor and major axes due to high stresses at regions of reduced thickness as shown in Fig. 16. Hence, in pipes with low D/t values, deep randomly distributed widespread internal corrosion defects induce random possibilities of collapse modes which can deviate significantly from what is imposed by the initial ovality. For high D/t values, collapse is elastic, hence, the collapse mode shape is unaffected by the depth of the surface defects and it is similar to that of a defect-free pipe as shown in the Appendix.

It is important to note that the distribution and circumferential orientation of the defects are important for determining collapse pressure. If the spatial distribution of the defects is denser at the location of failure initiation, the collapse pressure is more reduced than for a pipe with a uniform distribution of defects for the same total defect surface area coverage. This observation agrees with Wang et al. (2018b) who showed that collapse pressure for a pipe with random spatial distribution of corrosion pits decreased with increase in mass loss for the same length of defect coverage. Furthermore, the circumferential orientation of the defects at the location of collapse initiation on the pipeline model will result in an increased reduction in the collapse pressure if the defect is located at the most compressed region of the pipe. This agrees with observation from a prior study (Netto et al., 2007) where it was reported that a change in the orientation of defect on a pipe with ovality such that the defect falls on the most compressed region resulted in a reduction of collapse pressure capacity.

To simplify the prediction of failure by localised buckling due to the random spatially distributed corrosion defects on the internal surface of pipelines, an empirical equation is developed in the current study by

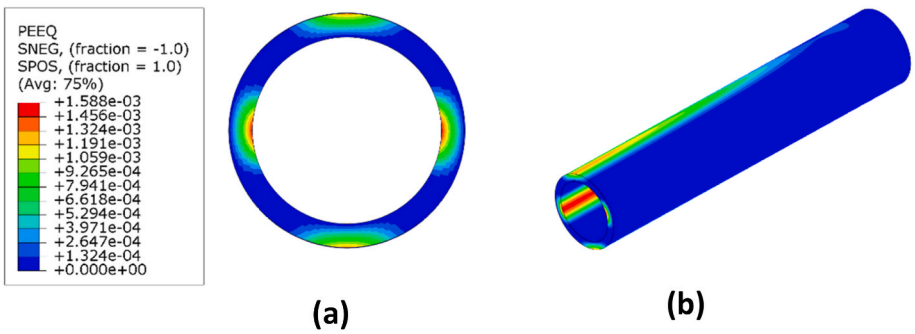

Fig. 14. Contour of effective plastic strain at the onset of collapse of a defect-free pipe with $D/t = 10$. (a) Cross-section of the pipe, and (b) 3D pipe geometry.

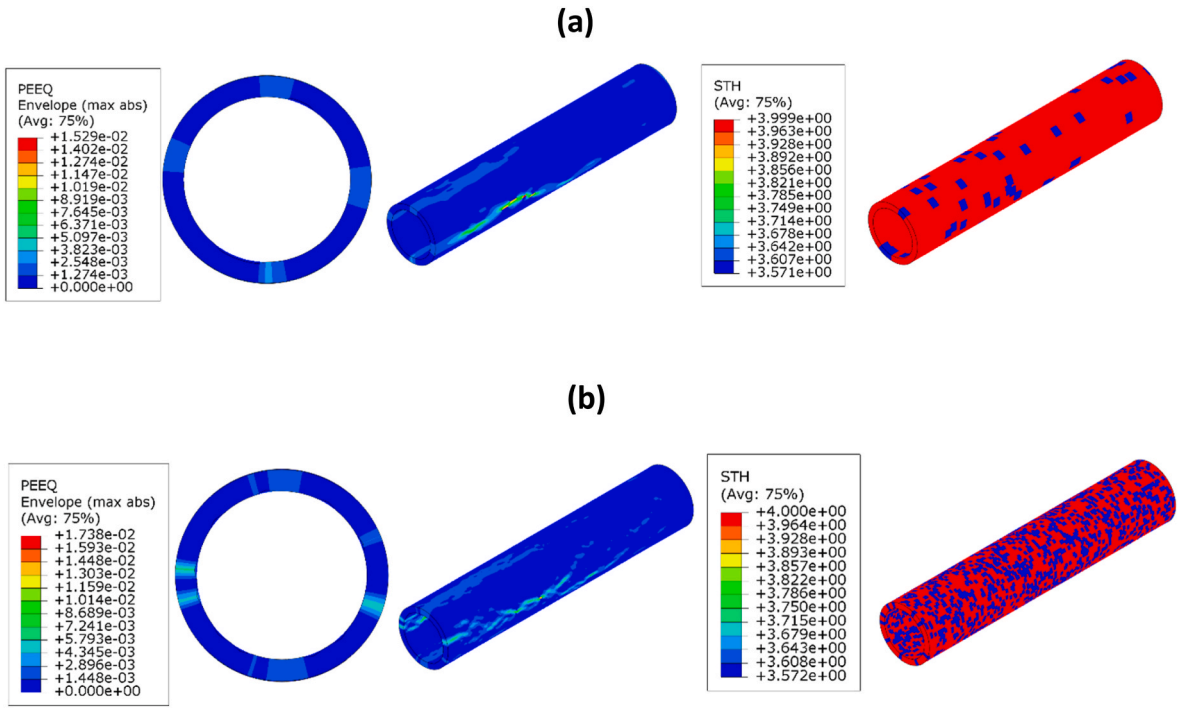

Fig. 15. Equivalent plastic strain at the onset of collapse and the corresponding defect coverage for (a) $\frac{D}{t} = 10, A_c = 0.1, \frac{c}{\pi D_i} = 0.05, \frac{d}{t} = 0.1$ and (b) $\frac{D}{t} = 10, A_c = 0.5, \frac{c}{\pi D_i} = 0.02, \frac{d}{t} = 0.1$.

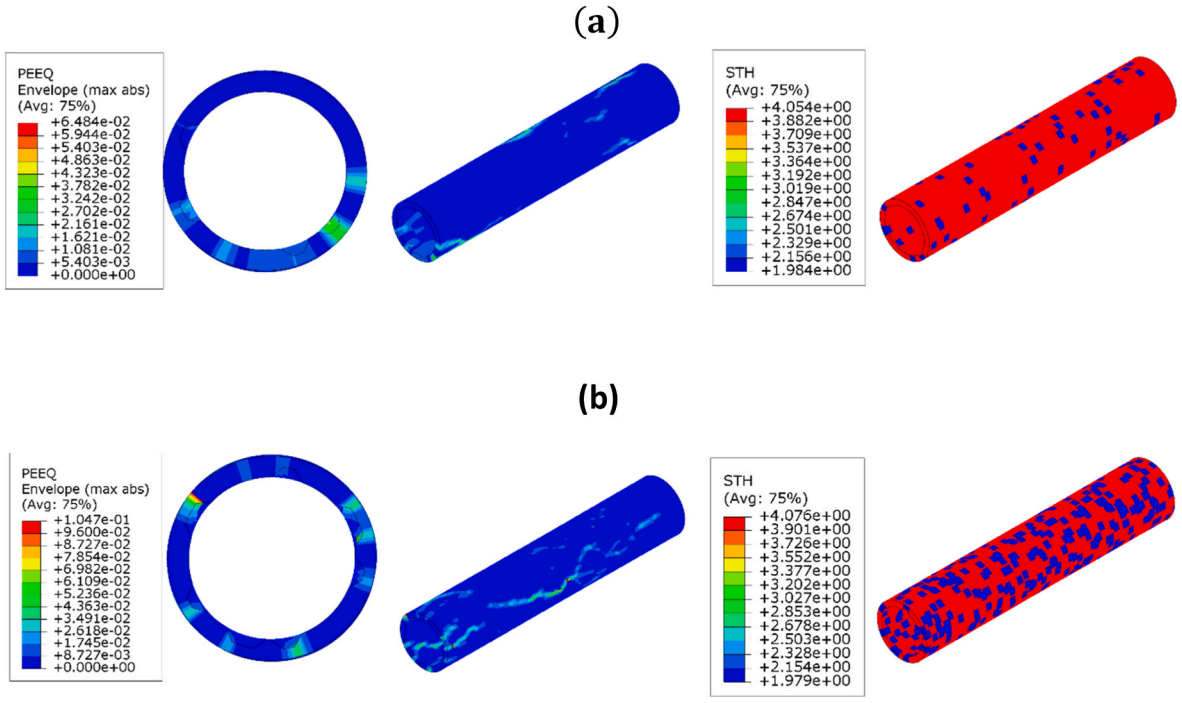

Fig. 16. Equivalent plastic strain at the onset of collapse and the corresponding defect distribution indicating significant effect of high relative defect depth on collapse mode (a) $\frac{D}{t} = 10, A_c = 0.1, \frac{c}{\pi D_i} = 0.04, \frac{d}{t} = 0.5$, and (b) $\frac{D}{t} = 10, A_c = 0.4, \frac{c}{\pi D_i} = 0.04, \frac{d}{t} = 0.5$..

nonlinear regression analysis of the FEA results (see section 3.6). This equation takes account of the inherent randomness of the defects.

3.6. Non-linear regression analysis

Based on the results of the parametric study, an empirically enhanced model for predicting the normalised collapse pressure was developed using non-linear regression analysis. The empirical model was chosen to be in the form of a knock-down factor that can be applied to the collapse pressure of a defect-free pipe to obtain the collapse pressure for a pipe with randomly distributed internal corrosion defects. The knock-down factor developed is a function of the significant defect geometric parameters (depth and total surface area of coverage of defects) observed from the simulation results. In total 505 design points were utilised for the regression analysis. The model was designed such that zero-coverage area and/or depth of defects sets the knock-down factor to 1. An exact convergence of the predictions to the collapse pressure of an intact pipeline for zero defect coverage area and/or depth cannot be achieved with a linear regression model even with the consideration of all the possible interactions amongst the parameters. The significance of the parameters can be easily observed from a simple linear regression analysis which includes all the parameters considered in the study. An exponential form of the knock-down factor is chosen as it also has the advantage of being able to be scaled as required to incorporate both linear and non-linear effects as observed in the results from the parametric study (see Figs. 10 and 12).

The regression model is given by;

$$\frac{P_{cor}}{P_c} = e^{A_c^{b_1} \times \left(\frac{d}{t}\right)^{b_2} \times b_3} \tag{8}$$

where b_j ($j = 1, 2, 3$) are the model nondimensional coefficients given in Table 2 for the range of values of defect geometric parameters considered in this study.

As shown in Figs. 8 and 9 the effects of D/t and $c/\pi D_i$ on the normalised collapse pressure of pipelines with randomly distributed internal corrosion defects are considerably less significant compared to the effects of A_c and d/t and including them in the regression model would yield no significant benefits. As a result, the model is a function of only A_c and d/t. It is important to note that the collapse pressure of the corresponding surface defect-free pipeline, P_c, is a function of the diameter-to-thickness ratio D/t, see eqn. (6) and Fig. 5. A model based on exponentials ensures that P_{cor} equals P_c when any of the defect geometric parameters are set to zero. The model coefficients and statistical details of the regression fit and are presented in Table 2 and the 95% confidence interval bar chart for the model coefficients is shown in Fig. 17.

The relative collapse pressures predicted by the model (8) using the model constants given in Table 2 are compared with the 505 different finite element predictions covering all values of D/t, d/t, $c/\pi D_i$, and A_c considered in this study as shown in Fig. 18, while the distribution of the percentage error of the model prediction is shown in Fig. 19. We note that the model has a mean absolute error below 3% for the 505 reference FEA results. The developed model accounts for 97.6% ($R^2 = 0.952$, see

Table 2
Non-linear regression model fitting constants.

	Estimated coefficients		
	b_1	b_2	b_3
Mean	0.8835	1.1149	−2.9424
Standard deviation	0.0173	0.0180	0.0856

Mean Absolute Error = 2.75%.
Maximum Absolute Error = 13.31%.
Root mean squared error = 0.0268.
R-Squared: 0.952.
p-value = 0.

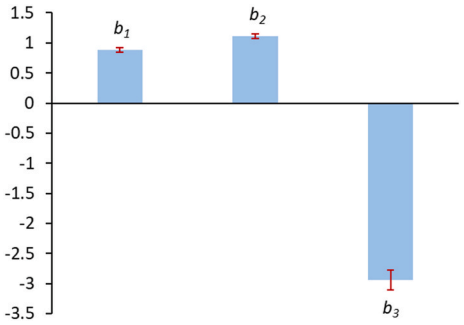

Fig. 17. 95% confidence intervals for the empirical model coefficients.

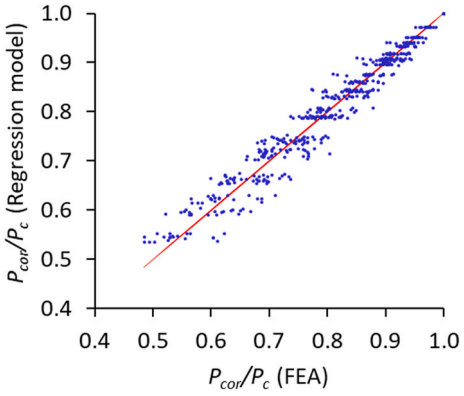

Fig. 18. Empirical model predicted normalised collapse pressure vs normalised collapse pressure from parametric FEA study.

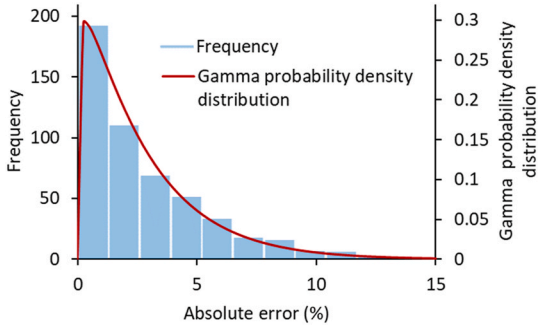

Fig. 19. Frequency distribution and gamma distribution fit of empirical model absolute errors.

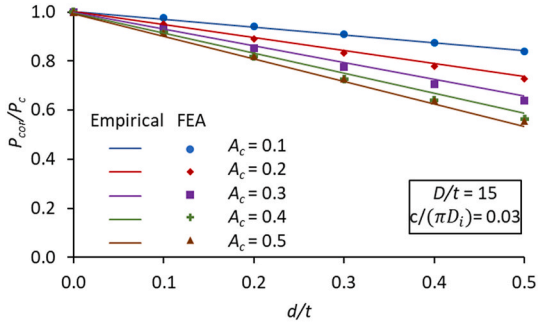

Fig. 20. Comparison of empirical model predicted normalised collapse pressure and the corresponding results from FE simulation.

Table 2) of the variations in the simulation data utilised. The empirical model (8) can be used for performing reliability analysis for predicting the failure of pipelines subject to evolving corrosion defects on the internal surface based on the assumption that the defects can be adequately represented by a mean size and depth removing the need for computationally intensive FEA.

Fig. 20 shows that the empirical model predictions of the relative collapse pressures are in very good agreement with the finite element results for the range of relative coverage and depth considered in this study.

It is to be noted that only randomly spatially distributed widespread corrosion defects of uniform geometry were considered in this paper for the API 5 L X65 pipeline. The developed model is for materials that exhibit linear hardening and may not suffice for prediction for other material types with different strain hardening response. Furthermore, corrosion defects on real pipeline may not be square in shape and may be of different shapes and geometry than what has been considered here in. FE Models with the exact expected shape of defect were not analysed for the parametric study because of the high mesh density and consequent computation resources that would be required for such simulations. However, future work would look at the effect of the statistical parameters such as mean and variance of the defect geometry on the collapse pressure of corroding pipelines. Furthermore, only internal corrosion has been considered in this work, however, there is a possibility of external widespread or localised corrosion defects to develop when spalling of the pipeline external coating occurs – a combined consideration of the effect of both internal and external random multiple defects would provide a more robust basis for longer term strength assessment of subsea pipelines.

4. Concluding discussion

This work investigated the effects of the geometrical properties and coverage extent of widespread internal pitting corrosion with random spatial distribution on pipeline collapse pressure. Shell finite element S4R from the Abaqus elements library was utilised to build the FE models for the investigation after confirming the computation efficiency superiority of the shell elements to the solid element (C3D8R), and accuracy against the solid element-based models and analytical results for pipes with diameter-to-thickness ration in range $10 \leq D/t \leq 50$. The FE models built with the shell element were validated for use in the current investigation by comparing the results to prior research of Netto et al. (2007) and Sakakibara et al. (2008).

The effect of random spatially distributed internal corrosion defects on collapse pressure is investigated for the first time by nonlinear finite analysis. The collapse pressure is determined for a wide range of diameter-to-thickness ratio D/t, relative surface area coverage of the defect A_c, relative defect length $\frac{c}{\pi D_i}$, and relative defect depth $\frac{d}{t}$. A robust empirical model capable of accurately predicting the effect of the defect geometric parameters on the collapse pressure is developed. Based on the results, the following conclusions can be drawn:

1. The normalised collapse pressure decreases almost linearly with increasing relative corrosion defect depth.
2. The normalised collapse pressure decreases with increasing relative coverage area of the defect A_c until $A_c = 0.4$, beyond which the surface coverage area has no significant effect on the collapse pressure.
3. The diameter-to-thickness D/t and relative length of the corrosion defects ($c/\pi D_i$) do not have significant effects on the normalised collapse pressure of the pipelines compared to the effect of relative surface area coverage and depth.
4. The collapse mode shape is dictated by a combination of the initial out-of-roundness imperfection imposed and geometric properties of the pipe and defects. At $D/t \leq 20$, deep defect depths ($d/t \geq 0.3$) can have a significant effect of the collapse mode shape. However, for $D/t \geq 30$ the defect depth has no significant influence on the collapse mode and the initial out-of-roundness imperfection dictates collapse mode. In all instances, the relative defect coverage has no significant effect of the collapse mode, but the circumferential orientation of the defect is important.
5. The normalised collapse pressure of a pipeline with evolving randomly spaced widespread internal corrosion defects can be approximated as a function of relative defect depth and defect coverage.

CRediT authorship contribution statement

Michael Olatunde: Formal analysis, Investigation, Methodology, Validation, Writing – original draft. **Srinivas Sriramula:** Conceptualization, Methodology, Supervision, Project administration, Writing – original draft, Writing – review & editing. **M. Amir Siddiq:** Conceptualization, Methodology, Supervision, Writing – original draft, Writing – review & editing. **Alfred R. Akisanya:** Conceptualization, Methodology, Supervision, Writing – original draft, Writing – review & editing.

Declaration of competing interest

The authors declare that they have no known competing financial interests or personal relationships that could have appeared to influence the work presented in this paper. However, we acknowledge the research funding by Chevron through its Anchor Partnership with the UK National Decommissioning Centre (NDC). We also acknowledge funding and in-kind support from the Net Zero Technology Centre and the University of Aberdeen through their partnership with the UK National Decommissioning Centre.

Data availability

No data was used for the research described in the article.

Acknowledgements

This research is funded by Chevron through its Anchor Partnership with the UK National Decommissioning Centre (NDC). We also acknowledge funding and in-kind support from the Net Zero Technology Centre and the University of Aberdeen through their partnership with the UK National Decommissioning Centre. The authors are grateful for helpful discussions with Dr Alethea Madgett of NDC.

Appendix. Effect of the defect geometric parameters, $A_c, c/\pi D_i, d/t$ and D/t, on collapse mode shape and orientation

Parameter						
A_c	$\frac{D}{t}=10,\ A_c=0.1,\ \frac{c}{\pi D}=0.02,\ \frac{d}{t}=0.1$	$\frac{D}{t}=10,\ A_c=0.5,\ \frac{c}{\pi D}=0.02,\ \frac{d}{t}=0.1$	$\frac{D}{t}=20,\ A_c=0.1,\ \frac{c}{\pi D}=0.02,\ \frac{d}{t}=0.1$	$\frac{D}{t}=20,\ A_c=0.5,\ \frac{c}{\pi D}=0.02,\ \frac{d}{t}=0.1$	$\frac{D}{t}=30,\ A_c=0.1,\ \frac{c}{\pi D}=0.02,\ \frac{d}{t}=0.1$	$\frac{D}{t}=30,\ A_c=0.5,\ \frac{c}{\pi D}=0.02,\ \frac{d}{t}=0.1$
$c/\pi D$	$\frac{D}{t}=10,\ A_c=0.1,\ \frac{c}{\pi D}=0.02,\ \frac{d}{t}=0.1$	$\frac{D}{t}=10,\ A_c=0.5,\ \frac{c}{\pi D}=0.05,\ \frac{d}{t}=0.1$	$\frac{D}{t}=20,\ A_c=0.1,\ \frac{c}{\pi D}=0.02,\ \frac{d}{t}=0.1$	$\frac{D}{t}=20,\ A_c=0.1,\ \frac{c}{\pi D}=0.05,\ \frac{d}{t}=0.1$	$\frac{D}{t}=30,\ A_c=0.1,\ \frac{c}{\pi D}=0.02,\ \frac{d}{t}=0.1$	$\frac{D}{t}=30,\ A_c=0.1,\ \frac{c}{\pi D}=0.05,\ \frac{d}{t}=0.1$
d/t	$\frac{D}{t}=10,\ A_c=0.1,\ \frac{c}{\pi D}=0.02,\ \frac{d}{t}=0.1$	$\frac{D}{t}=10,\ A_c=0.1,\ \frac{c}{\pi D}=0.02,\ \frac{d}{t}=0.5$	$\frac{D}{t}=20,\ A_c=0.1,\ \frac{c}{\pi D}=0.02,\ \frac{d}{t}=0.1$	$\frac{D}{t}=20,\ A_c=0.1,\ \frac{c}{\pi D}=0.02,\ \frac{d}{t}=0.5$	$\frac{D}{t}=30,\ A_c=0.1,\ \frac{c}{\pi D}=0.02,\ \frac{d}{t}=0.1$	$\frac{D}{t}=30,\ A_c=0.1,\ \frac{c}{\pi D}=0.02,\ \frac{d}{t}=0.5$
D/t	$\frac{D}{t}=10,\ A_c=0.5,\ \frac{c}{\pi D}=0.02,\ \frac{d}{t}=0.5$	$\frac{D}{t}=30,\ A_c=0.1,\ \frac{c}{\pi D}=0.02,\ \frac{d}{t}=0.5$	$\frac{D}{t}=50,\ A_c=0.5,\ \frac{c}{\pi D}=0.02,\ \frac{d}{t}=0.5$			

References

American Petroleum Institute, 2016. Fitness for service. In: API 579-1. https://webstore.ansi.org/standards/asme/api579asmeffs2016#DRM.

Assanelli, A.P., Toscano, R.G., Johnson, D.H., Dvorkin, E.N., 2000. Experimental/numerical analysis of the collapse behavior of steel pipes. Eng. Comput. 17 (4), 459–486. https://doi.org/10.1108/02644400010334856.

Bureau Veritas, 2018. Decommissioning on the UK Continental Shelf-An Overview of Regulations. www.decomnorthsea.com.

Chen, B.Q., Zhang, X., Guedes Soares, C., 2022. The effect of general and localized corrosions on the collapse pressure of subsea pipelines. Ocean Eng. 247, 110719 https://doi.org/10.1016/j.oceaneng.2022.110719.

Corona, E., Kyriakides, S., 1988. On the collapse of inelastic tubes under combined bending and pressure. Int. J. Solid Struct. 24 (5), 505–535. https://doi.org/10.1016/0020-7683(88)90005-4.

Crisfield, M.A., 1981. A fast incremental/iteration solution procedure that handles `Snap-Through'. Comput. Struct. 13 (1–3), 55–62. https://doi.org/10.1016/0045-7949(81)90108-5.

De Winter, P.E., 1981. Deformation capacity of steel tubes in deep water. Offshore Technology Conference. https://doi.org/10.4043/4035-MS. OnePetro.

Dessault-Systemes, 2019. *Abaqus/CAE 2020* (Build ID:2019_09_13-18.49.31.163176). Dasault Systemes Simulia Corp.

Det Norske Veritas, 2012. Offshore Standard, DNV-OS-F101: Submarine Pipeline Systems. http://www.dnv.com.

Fallqvist, B., 2009. Collapse of Thick Deepwater Pipelines Due to Hydrostatic Pressure. Royal Institute of Technology.

Gong, S.-F., Ni, X.-Y., Bao, S., Bai, Y., 2013. Asymmetric collapse of offshore pipelines under external pressure. Ships Offshore Struct. 8 (2), 176–188. https://doi.org/10.1080/17445302.2012.691273.

Hauch, S., Bai, Y., 2000. Bending moment capacity of pipes. Offshore Mechanical and Arctic Engineering122 122 (4), 243–353. https://doi.org/10.1115/1.1314866.

He, T., Duan, M., An, C., 2014. Prediction of the collapse pressure for thick-walled pipes under external pressure. Appl. Ocean Res. 47, 199–203. https://doi.org/10.1016/j.apor.2014.05.006.

Jin, B.-H., 2016. Collapse Strength of Thick-Walled Steel Pipe Considering Post-Buckling Behavior. Seoul National University.

Ju, G.T., Kyriakides, S., 1992. Bifurcation and localization instabilities in cylindrical shells under bending—II. Predictions. Int. J. Solid Struct. 29 (9), 1143–1171. https://doi.org/10.1016/0020-7683(92)90140-O.

Kara, F., Navarro, J., Allwood, R.L., 2010. Effect of thickness variation on collapse pressure of seamless pipes. Ocean Eng. 37 (11–12), 998–1006. https://doi.org/10.1016/j.oceaneng.2010.03.014.

Klever, F.J., 1992. Burst strength of corroded pipe: flow stress revisited. Offshore Technology Conference. https://doi.org/10.4043/7029-MS.

Li, T., Xie, P., Li, X., 2022. Collapse of medium-thick-walled pipes with multi-oval defects under external pressure. Ocean Eng. 258, 111621. https://doi.org/10.1016/j.oceaneng.2022.111621.

Liang, H., Zhou, J., Lin, J., Jin, F., Xia, F., Xue, J., Xu, J., 2020. Buckle propagation in steel pipes of ultra-high strength: experiments, theories and numerical simulations. Acta Mech. Solida Sin. 33 (4), 546–563. https://doi.org/10.1007/s10338-019-00148-w.

Mansoori, H., Mirzaee, R., Esmaeilzadeh, F., Vojood, A., Dowrani, A.S., 2017. Pitting corrosion failure analysis of a wet gas pipeline. Eng. Fail. Anal. 82, 16–25. https://doi.org/10.1016/j.engfailanal.2017.08.012.

MATLAB, 2021. The MathWorks Inc. version 9.10.0.1602886 (R2021a).

Murer, N., Buchheit, R.G., 2013. Stochastic modeling of pitting corrosion in aluminum alloys. Corrosion Sci. 69, 139–148. https://doi.org/10.1016/j.corsci.2012.11.034.

Netto, T.A., 2009. On the effect of narrow and long corrosion defects on the collapse pressure of pipelines. Appl. Ocean Res. 31, 75–81. https://doi.org/10.1016/j.apor.2009.07.004.

Netto, T.A., 2010. A simple procedure for the prediction of the collapse pressure of pipelines with narrow and long corrosion defects - correlation with new experimental data. Appl. Ocean Res. 32 (1), 132–134. https://doi.org/10.1016/j.apor.2009.12.007.

Netto, T.A., Ferraz, U.S., Botto, A., 2007. On the effect of corrosion defects on the collapse pressure of pipelines. Int. J. Solid Struct. 44 (22–23), 7597–7614. https://doi.org/10.1016/j.ijsolstr.2007.04.028.

ODU OPRED BEIS, 2018. Guidance Notes: Decommissioning of Offshore Oil and Gas Installations and Pipelines. https://www.gov.uk/beis.

Ramasamy, R., Tuan Ya, T.M.Y.S., 2014. Nonlinear finite element analysis of collapse and post-collapse behaviour in dented submarine pipelines. Appl. Ocean Res. 46, 116–123. https://doi.org/10.1016/j.apor.2014.02.007.

Sadowski, A.J., Fajuyitan, O.K., Wang, J., 2017. A computational strategy to establish algebraic parameters for the Reference Resistance Design of metal shell structures. Adv. Eng. Software 109, 15–30. https://doi.org/10.1016/j.advengsoft.2017.02.012.

Sadowski, A.J., Rotter, J.M., 2013. Solid or shell finite elements to model thick cylindrical tubes and shells under global bending. Int. J. Mech. Sci. 74, 143–153. https://doi.org/10.1016/j.ijmecsci.2013.05.008.

Sakakibara, N., Kyriakides, S., Corona, E., 2008. Collapse of partially corroded or worn pipe under external pressure. Int. J. Mech. Sci. 50 (12), 1586–1597. https://doi.org/10.1016/j.ijmecsci.2008.10.006.

Seber, G.A.F., Wild, C.J., 2003. Nonlinear Regression, vol. 62. John Wiley & Sons, Hoboken. New Jersey, p. 1238, 63.

Stanley, G.M., 1985. Continuum-based Shell Elements. Stanford University.

Valor, A., Caleyo, F., Alfonso, L., Rivas, D., Hallen, J.M., 2007. Stochastic modeling of pitting corrosion: a new model for initiation and growth of multiple corrosion pits. Corrosion Sci. 49 (2), 559–579. https://doi.org/10.1016/j.corsci.2006.05.049.

van den Berg, G., 1995. A Finite Strain Shell Model for the Analysis of Moderately Thick-Walled Tubes.

van Keulen, F., 1994. On Refined Triangular Plate and Shell Elements. Delft University of Technology.

Wang, H., Yu, Y., Yu, J., Duan, J., Zhang, Y., Li, Z., Wang, C., 2018a. Effect of 3D random pitting defects on the collapse pressure of pipe — Part I: experiment. Thin-Walled Struct. 129, 512–526. https://doi.org/10.1016/j.tws.2018.04.015.

Wang, H., Yu, Y., Yu, J., Jin, C., Zhao, Y., Fan, Z., Zhang, Y., 2018b. Effect of 3D random pitting defects on the collapse pressure of pipe — Part II: numerical analysis. Thin-Walled Struct. 129, 527–541. https://doi.org/10.1016/j.tws.2018.04.015.

Wang, R., Shenoi, A.R., 2019. Experimental and numerical study on ultimate strength of steel tubular members with pitting corrosion damage. Mar. Struct. 64, 124–137. https://doi.org/10.1016/j.marstruc.2018.11.006.

Witek, M., 2021. Structural integrity of steel pipeline with clusters of corrosion defects. Materials 14 (4), 1–15. https://doi.org/10.3390/ma14040852.

Wu, H., Zhao, H., Li, X., Feng, X., Chen, Y., 2022. Experimental and numerical studies on collapse of subsea pipelines with interacting corrosion defects. Ocean Eng. 260 (112066) https://doi.org/10.1016/j.oceaneng.2022.112066.

Xue, J., Hoo Fatt, M., 2002. Buckling of a non-uniform, long cylindrical shell subjected to external hydrostatic pressure. Eng. Struct. 24, 1027–1034. https://doi.org/10.1016/S0141-0296(02)00029-9.

Yeh, M.K., Kyriakides, S., 1986. On the collapse of inelastic thick-walled tubes under external pressure. J. Energy Resour. Technol. 108 (1), 35–47. https://doi.org/10.1115/1.3231239.

Yu, J.-X., Han, M.-X., Duan, J.-H., Yu, Y., Sun, Z.-Z., 2019. A modified numerical calculation method of collapse pressure for thick-walled offshore pipelines. Appl. Ocean Res. 91, 101884 https://doi.org/10.1016/j.apor.2019.101884.

Zhang, X., Chen, B., Guedes Soares, C., 2020. Effect of non-symmetrical corrosion imperfection on the collapse pressure of subsea pipelines. Mar. Struct. 73, 102806 https://doi.org/10.1016/j.marstruc.2020.102806.

Zhang, X., Pan, G., 2020. Collapse of thick-walled subsea pipelines with imperfections subjected to external pressure. Ocean Eng. 213, 107705 https://doi.org/10.1016/j.oceaneng.2020.107705.